We are IntechOpen, the world's leading publisher of Open Access books
Built by scientists, for scientists

6,900
Open access books available

185,000
International authors and editors

200M
Downloads

154
Countries delivered to

Our authors are among the

TOP 1%
most cited scientists

12.2%
Contributors from top 500 universities

CLARIVATE ANALYTICS
BOOK CITATION INDEX
INDEXED

WEB OF SCIENCE™

Selection of our books indexed in the Book Citation Index
in Web of Science™ Core Collection (BKCI)

Interested in publishing with us?
Contact book.department@intechopen.com

Numbers displayed above are based on latest data collected.
For more information visit www.intechopen.com

Inter-Diffusion of Nickel and Palladium with Germanium

Adrian Habanyama and Craig M. Comrie

Additional information is available at the end of the chapter

Abstract

Nickel and palladium germanides are the most promising candidates for nano-electronic contact materials to active areas of germanium-based devices. Solid-state reactions were thermally induced in conventional thin film couples of the Ni/Ge and Pd/Ge systems in order to study the sequence of phase formation. By embedding a thin layer of tantalum or tungsten as an inert marker between coupling thin film layers and observing its movement during phase formation, the dominant diffusing species were identified and monitored. In the Ni/Ge system, Ni_5Ge_3 was the first phase to form followed by NiGe. The results showed that during Ni_5Ge_3 formation, Ni was the sole diffusing species. During NiGe formation, both Ni and Ge diffused with the Ge diffusion prominent during the early stages, while the later stage of growth was dominated by Ni diffusion. The only phases observed to form in the Pd/Ge system were PdGe and Pd_2Ge, the latter being the first. Palladium was the dominant diffusing species during both phase formations. Lateral diffusion couples were also prepared by the deposition of thick rectangular islands of germanium on to thin films of nickel and palladium. Several aspects of thermally induced lateral (as opposed to vertical) growth of phases were studied.

Keywords: thin film, inter-diffusion, ion beam analysis

1. Introduction

Silicon-based materials used in nano-electronics have been pushed to their physical limits because of the downscaling of devices to ever smaller dimensions and greater performance. Charge carriers have a greater mobility in germanium than in silicon; therefore, research work is being carried out to see if Ge can be used in place of Si in some niche metal-oxide semiconductor (MOS) applications [1, 2] for high performance.

The implementation of Ge-based technology in the nano-electronics industry requires the identification of appropriate materials for ohmic contacts to the active areas of a Ge-based device. Metal-silicides are used as ohmic contacts in silicon technology; metal-germanides are therefore being investigated so that they may be used in a similar way in Ge-based technology. A systematic study of the thermally induced reaction of a large number of transition metals with germanium substrates revealed that NiGe and PdGe are the most promising candidates for ohmic contacts in germanium-based technology [2, 3].

Some electronic properties of Ni/Ge and Pd/Ge junctions have been studied in previous work. Schottky barrier diodes have been used in many applications such as gates for metal-semiconductor field-effect transistors, opto-electronics as in solar cells and solid-state detectors [4–7]. Some of the previous research on the electronic properties of Ni/Ge junctions is the work reported by Peng et al. [8] on the I-V characteristics of Ni/Ge(100) Schottky barrier-based diodes. Peng et al. [8] also reported on some work in which Schottky contacts were rapidly anneal treated at 300–600°C, resulting in nickel germanide-induced strain. Differences in lattice parameters caused the orthorhombic structure of NiGe to induce some epitaxial tensile strain on substrates of Ge. This strain was explained to be a possible cause for an observed increase in Schottky barrier height as the temperature of annealing was raised. Hallstedt et al. [9] studied the phase transformation and sheet resistance of Ni on single crystalline SiGe(C) layer after annealing treatments at 360–900°C. The formation of crystalline Ni(SiGe) was completed at 400–450°C but the thermal stability decreased rapidly with increased Ge amount due to agglomeration (binding of primary particles leading to phase formation). This thermal behavior was shifted to higher annealing temperatures when carbon was incorporated, Ni (SiGeC) layers formed at 500–550°C after which there was Ge segregation to the underlying layer and carbon accumulation at the interface. Thanailakis et al. [10] were able to demonstrate how the Schottky barrier heights of as-deposited Ni/Ge(111) and Pd/Ge(111) are related to the Ge substrate density of surface states and the Ni or Pd work functions, respectively.

Apart from electrical properties, a thorough understanding of the solid-state interactions in metal-germanium systems is required in order to foresee and avoid problems that may be encountered during integration [the process of producing an integrated circuit (I.C.)]. Solid-state interactions in the Ni/Ge system have been extensively studied in the past [1, 2, 11–13], while the Pd/Ge system has received less attention [14–16]. The available reports agree on the second and final phase, NiGe for the Ni/Ge system but there is some disagreement on the first phase. A few researchers report hexagonal Ni_3Ge_2 as the first phase [11] but monoclinic Ni_5Ge_3 is generally agreed upon by most researchers as the first phase to form [1, 2, 12, 13] and it forms around 150°C. There is an agreement that Pd_2Ge is the first phase to be formed in the Pd/Ge system, the second and final phase to be formed is PdGe. The formation of these phases is generally reported to be sequential [4, 15] but PdGe has been reported to form before the end of Pd_2Ge formation [16]. **Table 1** summarizes the sample preparation, observed phase-formation sequences and some formation temperatures (where available) of the phases in the Ni/Ge and Pd/Ge systems, as reported by some previous researchers.

What is lacking in the previous research done in this area is a quantitative determination of the dominant diffusing species (DDS) during NiGe and PdGe formation and a comprehensive lateral diffusion study of the Ni/Ge and Pd/Ge systems. The DDS during first phase formation,

Sample preparation	Characterization techniques used	Phase formation	Refs.
Ge(111) wafers were cleaned by piranha (H_2O_2/H_2SO_4 = 1:3) before a Ni sputter deposition. Prior to the Ni deposition, the samples were dipped into dilute HF to remove any residual native oxide. A Ni film of about 100 Å thick was deposited onto the wafers at room temperature by sputtering. The base pressure was below 5×10^{-7} Torr and the deposition pressure was about 3×10^{-3} Torr.	Two annealing methods were used. The first method was rapid thermal annealing (RTA) at 400°C for 60 s in an N_2 ambient with a ramp rate of 30°C/s, while the other method was an in situ annealing process at 400°C for 30 min in the Ni sputtering chamber. Samples were characterized by 2D area X-ray diffraction (XRD) with Cu $K\alpha$ radiation and micro-Raman spectroscopy techniques. Cross-sectional transmission electron microscopy (TEM) was employed to study the surface morphology and the interfacial structure of the annealed films. Corresponding elemental information was determined using the energy dispersive X-ray spectrometry (EDS) technique in TEM.	According to the EDS analysis in TEM, two phases, NiGe and Ni_3Ge_2, were detected in the RTA method, whereas only the NiGe phase was observed at 400°C in the in situ annealing method.	Jin et al. [11]
Several substrate options were overviewed. Ge wet etch behavior was reported in a variety of acidic, basic, oxidizing, and organic solutions, widely used in the microelectronics industry. Modifications of the cleaning procedure suitable for Ge are discussed. The electrical data analyzed was from pMOS devices of 1–2 μm thick Ge on Si wafers.	This work provided an overview of some of the key processing issues for the fabrication of Ge pMOS devices and their impact on performance. Junction leakage behavior as a function of n-type doping, temperature, and electric field for Ge pMOS devices was analyzed.	NiGe germanide voids were reported to form in the active areas of the devices but the use of a two-step rapid thermal anneal (two-RTA) process was shown to suppress these defects.	Brunco et al. [1]
Metal films, nominally 30 nm thick, were deposited at room temperature by magnetron sputtering on substrates of crystalline Ge(001) and 200 nm amorphous germanium (a-Ge) over 100 nm SiO_2 on Si(001) wafers. The Ge substrates were cleaned with dilute HF (100:1). The base vacuum of the magnetron sputtering system was 1.3×10^{-7} Pa and the Ar pressure during deposition was maintained at 0.53 Pa.	Metal-Ge reactions were monitored in situ during ramp anneals at 3°C s^{-1} in a purified He atmosphere using time-resolved XRD, diffuse light scattering, and resistance measurements.	NiGe and PdGe phases appeared especially interesting: they exhibited the lowest sheet resistance, formed at low temperature, had limited sensitivity to oxidation and remained morphologically stable over a wide temperature range. The morphological degradation began at 580 and 550°C for NiGe and PdGe, respectively.	Gaudet et al. [2]
Thin films of 50 nm polycrystalline Ni were deposited by e-beam evaporation on 500 nm amorphous or polycrystalline germanium (a-Ge or p-Ge). The reactions were characterized by ex $situ$ and in situ XRD using the Bragg–Brentano geometry and a Cu $K\alpha$ source. Isothermal heat treatments were performed in situ	The first phase was carefully investigated by XRD and TEM. Samples at selected stages of reaction were taken out and analyzed ex $situ$ by long collection time XRD and examined by TEM both in plane view and cross-sectional samples.	The formation of NiGe was observed during deposition. Ni_5Ge_3 was then observed to form. It was shown that the growth of Ni_5Ge_3 and NiGe was simultaneous and not sequential, during isothermal annealing. Ni_5Ge_3 reached a critical thickness (around 10 nm) before NiGe was able to grow.	Nemouchi et al. [12]

Sample preparation	Characterization techniques used	Phase formation	Refs.
at temperatures between 150 and 190°C in vacuum in the 10^{-5} mbar range.			
100 nm of Ge was evaporated onto thermally oxidized Si wafer substrates, which were 75 mm in diameter. This was followed by a 400 nm deposition of room temperature Ni. The wafers were cleaned using a standard organic solvent and acid etch sequence.	Both temperature ramping and isothermal annealing were performed. Characterization was by XRD, cross-sectional TEM, 4-point kelvin resistance measurements and X-ray photoelectron spectroscopy (XPS).	The reaction path began with the consumption of Ni and Ge to form Ni_5Ge_3 and continued with the consumption of Ni_5Ge_3 and Ge to form NiGe in the temperature range, 200–300°C. NiGe was the terminal phase with agglomeration (in this case, being the segregation of Ge to the exposed surface) occurring at around 500°C.	Patterson et al. [13]
Ni films, 30 nm thick, were deposited at room temperature by magnetron sputtering on substrates of Ge(111), Ge(001), and 200 nm amorphous germanium (a-Ge) over 100 nm SiO_2 on Si(001) wafers. The Ge substrates were cleaned with dilute HF (100:1). The base vacuum of the magnetron sputtering system was 1.3×10^{-7} Pa and the Ar pressure during deposition was maintained at 0.53 Pa.	Ni/Ge reactions were monitored in situ during ramp anneals in a purified He atmosphere using time-resolved XRD, diffuse light scattering, and resistance measurements.	$Ni_5 Ge_3$ and NiGe appeared consecutively on Ge(111) while they grow simultaneously on a-Ge and Ge (001). Phase-formation temperatures depended strongly on the nature of the substrate being the lowest on a-Ge and the highest on Ge(111).	Gaudet et al. [14]
Samples were prepared by depositing 1000–3000 Å thick Pd films on large-area Ge(111) and Ge (100) substrates by an electron beam. The Ge wafers were etched in CP4, rinsed in deionized water, and immersed in a solution of HF. Pd was also evaporated on amorphous Ge layers evaporated on silicon oxide substrates. Heat treatment was performed both in vacuum and N_2.	The phases were identified by X-ray diffraction and grain size measurements were performed by X-ray diffraction line broadening. Rutherford Backscattering Spectroscopy (RBS) and RBS channeling measurements were also performed to study the structural phase orientation with respect to the substrate lattice.	The hexagonal Pd_2Ge phase was observed at 120°C. Orthorhombic PdGe was observed at higher temperatures and/or longer annealing times. The structure of the compounds was not significantly affected by the nature, either evaporated or single-crystal, of the germanium substrate; however, the kinetics, both for Pd_2Ge and for PdGe, were three to four times faster on amorphous Ge than on single-crystal Ge.	Majni et al. [15]
The substrates consisted of Ge (100), Ge(111), polycrystalline Ge wafers, and a 200 nm thick amorphous Ge film that was deposited on an SiO_2 wafer using thermal evaporation in a vacuum of 10^{-4} Pa. After a short HF dip (20 s), a 30, 100, or 150 nm thick Pd film was sputter deposited in an Ar atmosphere with a pressure of 5×10^{-1} Pa.	Samples were characterized by means of in situ XRD and laser light scattering (LLS). The kinetics of the Pd/Ge solid-state reaction was performed in which the thickness of the growing Pd germanides was monitored using in situ RBS.	The first germanide that is observed during the Pd/Ge solid-state reaction is the Pd_2Ge phase at 200°C This phase grows up to 270°C at which temperature, the entire Pd film was consumed. The Pd_2Ge phase then became the seeding layer for the growth of the PdGe phase which was stable up to its melting temperature of 725°C.	Knaepen [16]

Table 1. Summary of the sample preparation and observed phase-formation sequence and some formation temperatures (where available) of the phases in the Ni/Ge and Pd/Ge systems, as reported by some previous researchers.

that is, formation of Ni_3Ge_2 and Pd_2Ge, has been reported. Palladium is reported to be DDS during Pd_2Ge formation, contributing about two-third toward diffusion [17], while Ni appeared to be the sole moving species during the formation of the first nickel germanide phase, Ni_3Ge_2 [18]. The literature appears to be lacking in information regarding the diffusing species during the formation of subsequent phases in both the Pd/Ge and Ni/Ge systems. It has however been proposed that during NiGe formation in certain thin film configurations, Ge could be the DDS [19]. As mentioned earlier, NiGe and PdGe are the most promising candidates for ohmic contacts in germanium-based technology [2, 3].

The approach of our study, as presented in this chapter, is essentially twofold. Firstly, solid-state reactions were thermally induced in conventional nano-metric thin film couples of the Ni/Ge and Pd/Ge systems in order to study the sequence of phase formation in these two germanide systems. Conventional thin film couples were also used to identify and monitor the dominant diffusing species during the phase formation. By embedding a thin layer of tantalum (Ta) or tungsten (W) as an inert marker between coupling thin film Ni/Ge or Pd/Ge layers, the atomic transport across this marker layer could be monitored by observing the movement of the marker during phase formation. It is important, for device integrity, to identify the DDS during the formation of the respective germanides as this can influence their thermal stability. Excessive diffusion of the substrate element, in this case Ge, during germanide formation could result in overgrowth and bridging in devices, which would have a detrimental effect on their performance [20].

Secondly, lateral diffusion couples were prepared by the deposition of thick rectangular islands of one material on top of a much thinner film of another material. Upon annealing, the island-material would react with the underlying film through vertical diffusion. The natural phase-formation sequence of the system is followed up to the phase that has the highest proportion of island-material. At this point, the vertical diffusion gives way to lateral diffusion because there can be no further reaction between the island-material and the thin film material directly below it. The lateral diffusion may result in the phase that is most island-material rich to grow outward into the surrounding thin film. This phase would eventually reach a critical growth length where it would then give way to the lateral growth of other phases, simultaneous growth of a number of lateral phases of often observed. This multiple phase formation is not common in conventional thin film couples but is typical of bulk diffusion couples; therefore lateral diffusion couples offer a transition between these two types of behavior. The amount of material that is deposited in the island region of a lateral diffusion couple is relatively large. This allows one to carry out a more extensive investigation of phase formation and reaction kinetics than can be achieved using ordinary planar thin films. Bulk diffusion couples can be simulated using lateral diffusion structures because in the latter structures, phase formation could extend to length of around 100 μm [21]. In kinetic studies of thin film planar structures, the diffusion lengths are typically less than 0.5 μm. One can therefore study the transition from thin film to bulk diffusion couple behavior. The study of lateral diffusion couples is particularly well suited for dealing with the challenges of achieving the required lateral abruptness of semiconductor junctions. Various early techniques were developed to study lateral diffusion couples [22–31]. In later studies, microprobe-Rutherford backscattering spectrometry (μRBS) was used to study them [21, 32, 33]. The major advantage of this technique is its ability to give depth information.

2. Experimental summary

Conventional thin film couples for the Ni/Ge study were prepared using electron beam evaporation at a pressure of 10^{-7} Torr. The deposition technique used to prepare the thin film samples for the Pd/Ge study was sputtering at a pressure of 10^{-6} Torr. Ge(100) substrates were chemically cleaned in a procedure that ended with a 2% HF dip before being loaded for evaporation. The inert marker used for the Ni/Ge investigation was a 0.5 nm thick layer of Ta. The Pd/Ge marker study was carried out using a 0.3 nm thick layer of W. Since NiGe and PdGe phase formation takes place around 250–350°C, whereas Ta only begins to react with Ge at temperatures above 750°C and W does not appear to react with Ge at all (at least to temperatures of up to 900°C) [2], both Ta and W should remain chemically inert during the formation of the various germanide phases.

Instead of using the conventional approach, where different thermal anneals are performed on similar specimens after which the position of the marker is determined, we have performed the thermal anneal and measurement simultaneously using real-time Rutherford Backscattering Spectrometry (RBS). Using this method, only one sample can be used to monitor the position of the marker during the whole reaction process. In this way, one is able to identify the diffusing species more accurately because it eliminates the small variations that always exist between samples. Real-time RBS is able to determine any variations in the relative contributions of the diffusion of each atomic type as the reaction proceeds. RBS has the useful capacity of being able to give depth information of atomic composition thereby making it possible to monitor the position of the marker, between coupling layers, during phase formation. Real-time RBS data were collected during a ramped annealing rate of 2°C/min for the Ni/Ge system and a rate of 1°C/min for the Pd/Ge system. An ion beam of 2 MeV alpha particles was used to produce the RBS data, which were recorded in 30-s intervals during annealing. Statistical improvement of the results was achieved by grouping the data such that each group provided a statistically averaged spectrum within a temperature range of 4°C in the Ni/Ge investigation and 2°C in the Pd/Ge study. RUMP software [34] was used for the analysis of the RBS data. In a number of our figures, we use the thickness units of atoms/cm^2 because they are easier to work with in RBS-related studies of atomic diffusion than the conventional units of nm. The two units are interchangeable in that by dividing the values in atoms/cm^2 by the atomic concentration of a layer one gets a thickness in cm, which is then converted to nm.

For the Ni/Ge investigation, a single detector positioned at a backscattering angle of 165° was used and the sample was rotated by 50° with reference to the direction of the incident alpha particles, the depth resolution is improved in this way. The atomic masses of Ni and Ge are relatively close resulting in peak overlap between the Ni and Ge RBS spectra. This is more so if Ni is on the top of Ge because the atomic mass of Ni is smaller than that of Ge. Ordinarily, this would make the RBS analysis problematic but the Ni/Ge system only has two phases Ni$_5$Ge$_3$ and NiGe, which can be resolved using careful RUMP simulation. The Ni/Ge system, on the other hand, has the advantage that the small peak from the thin Ta marker is not close to the Ni or Ge peaks.

In the Pd/Ge system, Pd and Ge peaks do not overlap but the small peak of the W marker is close to the Pd peak. For this reason, the thickness of the Pd layer had been relatively small and it was necessary to mount a second RBS detector. The first detector was placed at a scattering angle of 165° and the sample normal rotated by 30° to the He$^+$ beam direction toward the detector. With this geometry, it was possible to separate the W marker signal from the Pd signal, but the depth resolution was compromised. A second detector was therefore placed at a scattering angle of −135°, which produced a scattering outgoing beam angle of 75° with respect to the normal of the surface. This geometry of the second detector improved the depth resolution for determining the thickness of various layers of phases; however, the second detector could not determine the position of the W marker because the geometry resulted in an overlap between the Pd and W peaks. The spectrum from the second detector was therefore used to determine the thicknesses of the various palladium germanide phases, while that from the first detector establish the depth of the W marker in the layers. Combining the information obtained from the two detectors in this way enabled the thickness of the various phases to be measured with reasonable confidence, while at the same time determining the depth of the marker in the sample.

The lateral diffusion couples were prepared by electron beam evaporation at a base pressure in the low 10^{-5} Pa range. Thermally oxidized single crystal silicon wafers with a (100) crystal orientation were used as substrates in all studies. The reaction of SiO_2 with Ge, Ni, or Pd was insignificant at the annealing temperatures used; hence, the substrates were "inert." A thin film of one material was deposited first. Without breaking the vacuum, an ordinary silicon wafer with an array of 390×780 µm^2 rectangular windows (referred to as a silicon mask) made by photolithographic techniques and selective etching, was thereafter placed close to the surface of the thin film that was deposited first. A second material was then deposited through the rectangular windows in the silicon mask to form islands of the second material on thin films of the first material. After removing the samples from the evaporation chamber, they were cleaved into 12 parts, which were later annealed and analyzed.

The samples were examined using scanning electron microscopy (SEM) to distinguish the various reaction regions and measure their diffusion lengths. Representative samples were selected for further analysis by µRBS. The distribution of elements as a function of lateral position was obtained using µRBS. This technique also provided information regarding the elemental distribution as a function of depth and the thickness of the films. 2 MeV alpha particles were focused to a beam size of about 1×1 µm using a nuclear microprobe and scanned across an area of the samples, which was chosen in such a way as to include all reaction regions identified using SEM. The size of the scanned area was about 400×400 µm^2. The samples were placed in such a way that the alpha beam scanned parallel to the edge of the original interface between the island and surrounding film. This avoided any compositional variations along the line scanned by the beam. About 128 RBS spectra were collected along each line scanned and these were summed to improve statistics. About 128 lines were scanned parallel to the original island interface, which resulted in RBS data being recorded as a function of lateral position. RUMP simulation was used to analyze the data.

3. Results

3.1. Ni/Ge system

3.1.1. Thin film couples

The thin film sample used to investigate the relative contributions of each atomic species to the diffusion process in the Ni/Ge system was prepared with the configuration: Ge(100)/Ta (0.5 nm)/Ni(76.5 nm). If this sample configuration is annealed, one would expect to observe the Ta marker moving toward the surface, if Ni were the dominant diffusing species during the formation of Ni_5Ge_3. If Ge was the dominant diffusing species, then the marker would move into the sample away from the surface. **Figure 1** shows the real-time RBS results during a ramped anneal at a rate of 2°C/min.

Figure 1(a) shows a stacking up of RBS spectra obtained during the annealing as a function of temperature producing a "surface" plot. The small Ta marker peak is seen around channel 405. The Ni and Ge signals are at channels below the Ta channel position. The Ta marker moves to
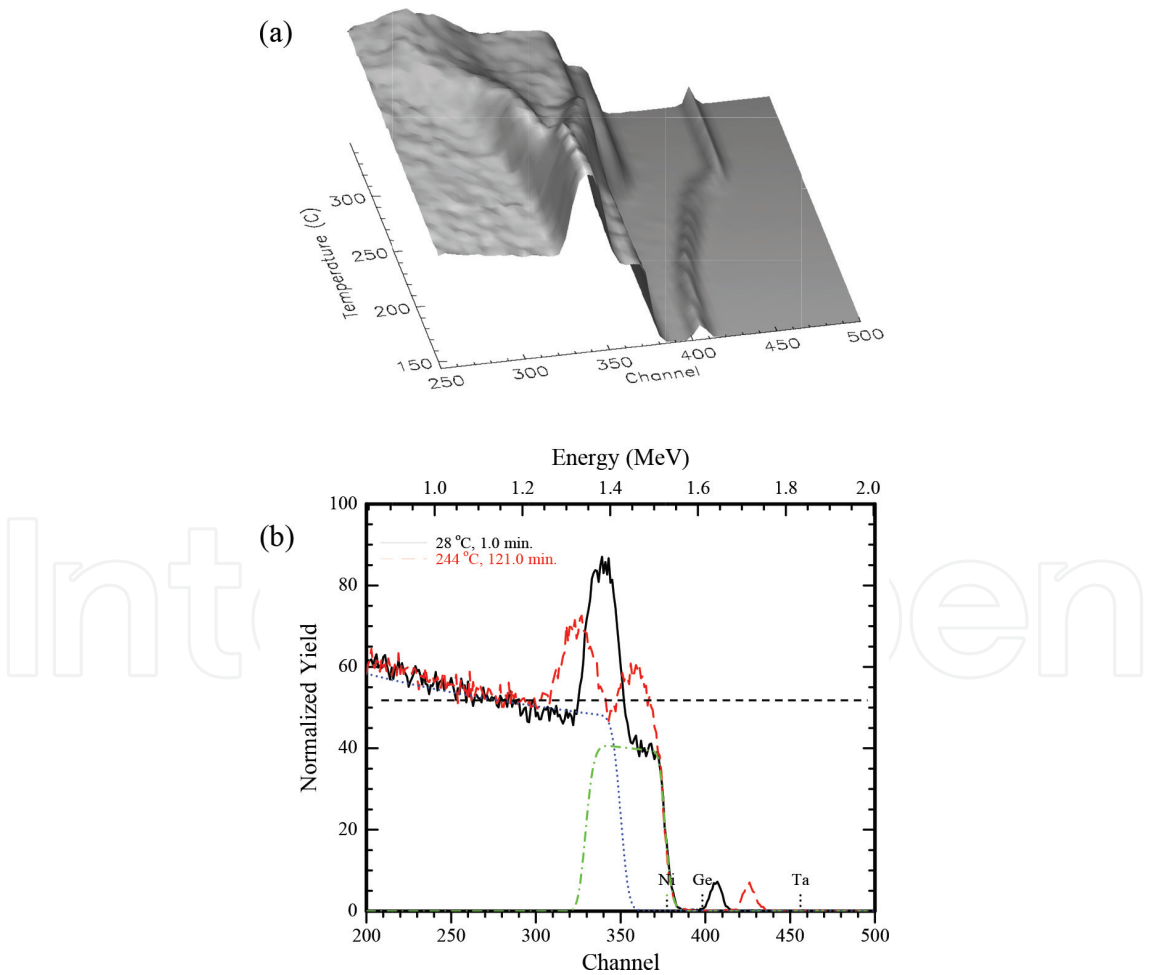
Figure 1. (a) Surface plot of RBS spectra obtained after the annealing of a Ge(100)/Ta/Ni sample at 2°C/min, the movement of the Ta marker to higher energies during the thermal anneal is clearly visible in the figure. (b) Individual as-deposited and 244°C RBS spectra with simulations showing the contribution of the Ni (lower dashed line) and Ge (dotted line).

higher channels as the temperature is increased indicating that Ni was the dominant diffusion species.

Figure 1(b) shows a spectrum from the as-deposited sample, which is similar in form to the front spectrum in **Figure 1(a)**, since there is a very little reaction below 150°C. **Figure 1(b)** also shows a spectrum, which was captured during the reaction around 244°C. The Ge, Ni, and Ta surface positions are indicated in the figure. The separate contributions of the Ge and Ni peaks to the spectrum from the as-deposited sample were simulated using RUMP and are also shown in the figure. It can be seen that the Ge and Ta signals appear at lower positions than their surface positions because there is a layer of Ni above them. The shoulder at the high energy end of the Ni signal is at the surface position as would be expected. The peak around channel 340 is due to the overlap between the back of the Ni signal and the front of the Ge signal. The Ni diffuses deeper into the sample as the reaction proceeds while the Ge diffuses toward the surface. This causes the overlap peak to split into two as seen in the spectrum collected at a temperature of 244°C.

An analysis of the individual RBS spectra indicated that the formation of Ni_5Ge_3 below the marker began around 155°C. As the reaction proceeded, the Ni_5Ge_3 phase continued to grow below the marker until around 200°C. When the Ni_5Ge_3 layer grew to a thickness of 14.2 nm, the NiGe phase started to appear below the marker between the Ge substrate and the Ni_5Ge_3 layer. As the temperature was increased, the two phases grew simultaneously. At around 265°C, about 55% of the Ni was consumed and at this point, the thickness of the layers of Ni_5Ge_3 and NiGe were 38.4 and 18.1 nm, respectively.

The Ta marker is observed to be at the surface position in the final spectra. Since, all the NiGe formed was below the marker, it is obvious that the marker movement was solely due to the growth of Ni_5Ge_3. We therefore conclude that Ni was the only diffusing species during the formation of Ni_5Ge_3. If there had been any Ge diffusion, then the Ta marker would not have been at the surface position after all the Ni had been consumed.

Since the growth of NiGe was below the marker, it was not possible to determine the dominant diffusing species during the formation of this phase. A sample with a different configuration was needed in order to study the relative diffusion of Ni and Ge during the formation of the phase NiGe. The configuration of the sample prepared for investigating the growth of NiGe was: Ge(100)/Ta(0.5 nm)/Ge(49 nm)/Ni(47 nm). Upon annealing this sample, there should be a reaction between Ni and Ge deposited on top of the Ta. **Figure 2** is a schematic diagram illustrating the various stages of this reaction.

As illustrated in **Figure 2(b)**, the sample was designed to make sure that after all the deposited Ge was consumed forming Ni_5Ge_3, there would still remain some Ni above the marker (about 7.5 nm of Ni). This Ni_5Ge_3 cannot be converted into NiGe while there is still some unreacted Ni above the marker. The only way that the reaction can continue is by the Ni above the marker reacting with Ge below the marker. Since we have established that Ni is the only diffusing species during the formation of Ni_5Ge_3, we would expect Ni to diffusing across the marker presumably to form Ni_5Ge_3 below, this is illustrated in **Figure 2(c)**. The abundance of Ge below the marker means that the Ni_5Ge_3 below would react with Ge thereby converting into the more Ge rich phase NiGe, this is illustrated in **Figure 2(d)**. One can then study the diffusing species
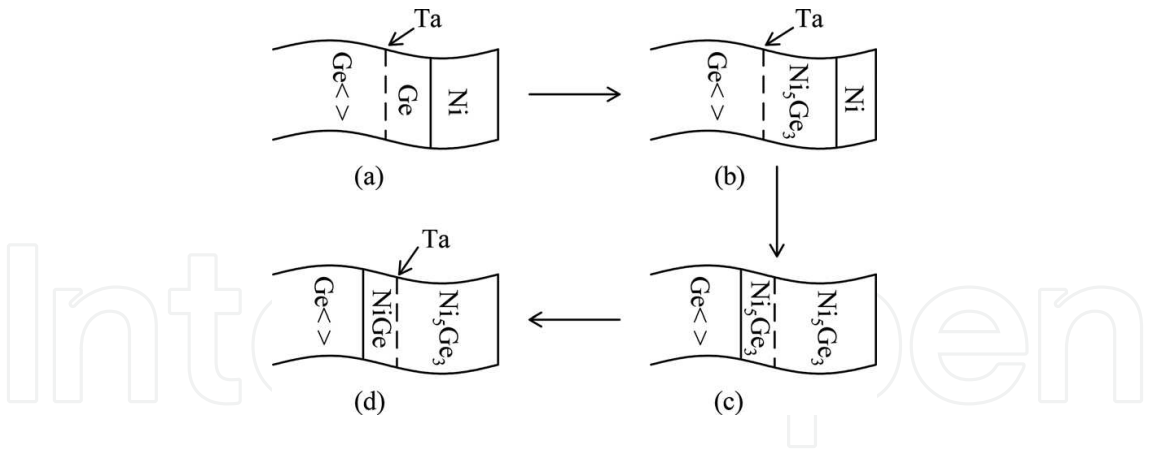
Figure 2. Schematic diagram showing the sample configuration used to determine the dominant diffusing species during NiGe formation. Upon heating, Ni first reacts with the Ge deposited on top of the marker and then the remaining Ni, after all the Ge on top of the marker has been consumed, diffuses past the marker [35].

during the formation of NiGe by monitoring the marker movement as Ni_5Ge_3 is converted into NiGe. **Figure 3** shows the ramped real-time RBS results of the thickness evolution of each layer as a function of temperature, as analyzed using RUMP.
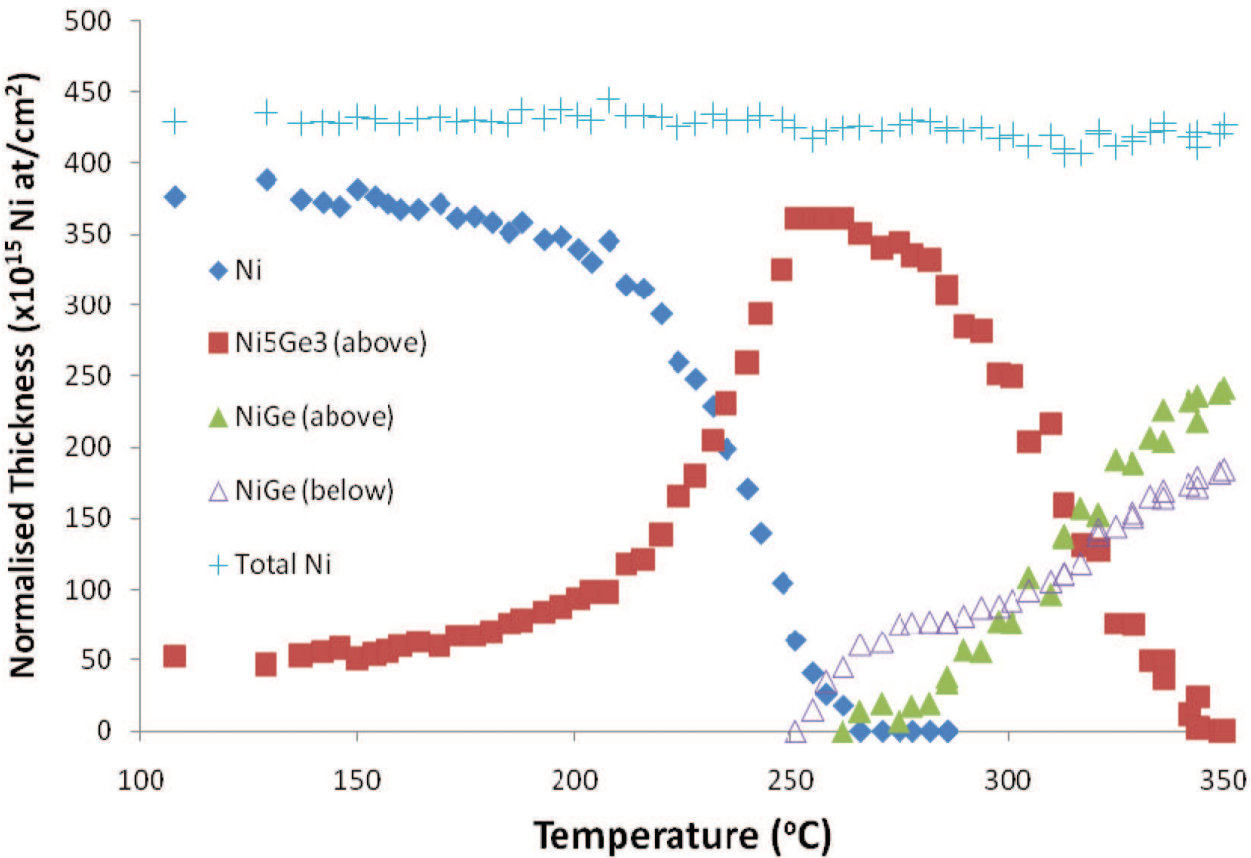
Figure 3. Experimental results showing the thickness of the various layers formed during the ramped annealing of the Ge(100)/ Ta/Ge/Ni sample. The thickness of each layer is expressed in Ni atoms/cm² for normalization. With this format, the total Ni thickness remains constant throughout the process making it easier to determine the relative proportion of each layer formed [35].

3.1.2. Lateral diffusion couples

The lateral diffusion couples prepared with thick Ni islands on thin Ge films showed very limited lateral diffusion upon annealing. The reaction did not proceed beyond a certain point despite annealing at high temperatures and for long periods of times. The reaction region was too narrow to properly resolve and monitor, this is a qualitative indicator that Ni was not a DDS for lateral phase growth in the Ni/Ge system. The reverse configuration with Ge islands (200 nm thick) on Ni films (36 nm thick) showed substantial lateral diffusion indicating that Ge is the DDS during lateral phase growth in the Ni/Ge system. **Figure 4(a)** shows an optical micrograph of part of a Ge island on a sample that was annealed at 500°C for 2 h. The darkened rectangular area on the right end of the island is the area that was scanned with the nuclear microprobe. **Figure 4(b)** is an SEM micrograph covering the various reaction zones of the sample shown in **Figure 4(a)**.

There are five reaction regions observed in **Figure 4** and they are label from A to E. The region labeled A is the original Ge island region, while E is the region of the unreacted Ni film. The regions labeled from B to D are phase regions produced during the thermal annealing of the sample. There is no well-defined boundary seen in **Figure 4(b)** between the regions C and D but region D clearly appears coarser than region C.

Figure 5(a)–(d) shows the representative measured RBS spectra extracted from each of the four reaction regions A–D in the sample annealed at 500°C for 2 h, together with their RUMP simulations; thickness is in units of 10^{15} atoms/cm^2.

The simulations show that region A comprised of NiGe overlaid by unreacted Ge while regions B, C, and D consisted of exposed NiGe, Ni$_3$Ge$_2$, and Ni$_5$Ge$_3$, respectively. The original island interface is between the NiGe and Ni$_3$Ge$_2$ phases.

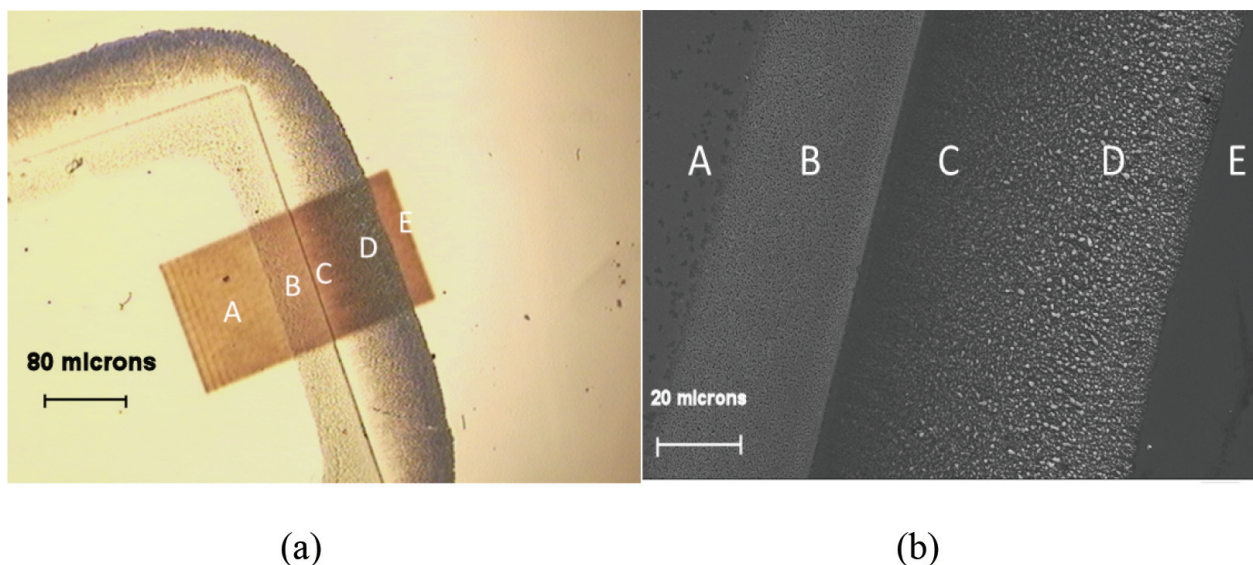(a)   (b)

Figure 4. (a) An image obtained using an optical microscope showing one end of an island after annealing at 500°C for 2 h. (b) A micrograph showing five regions obtained using SEM on the same island shown in (a) [36].
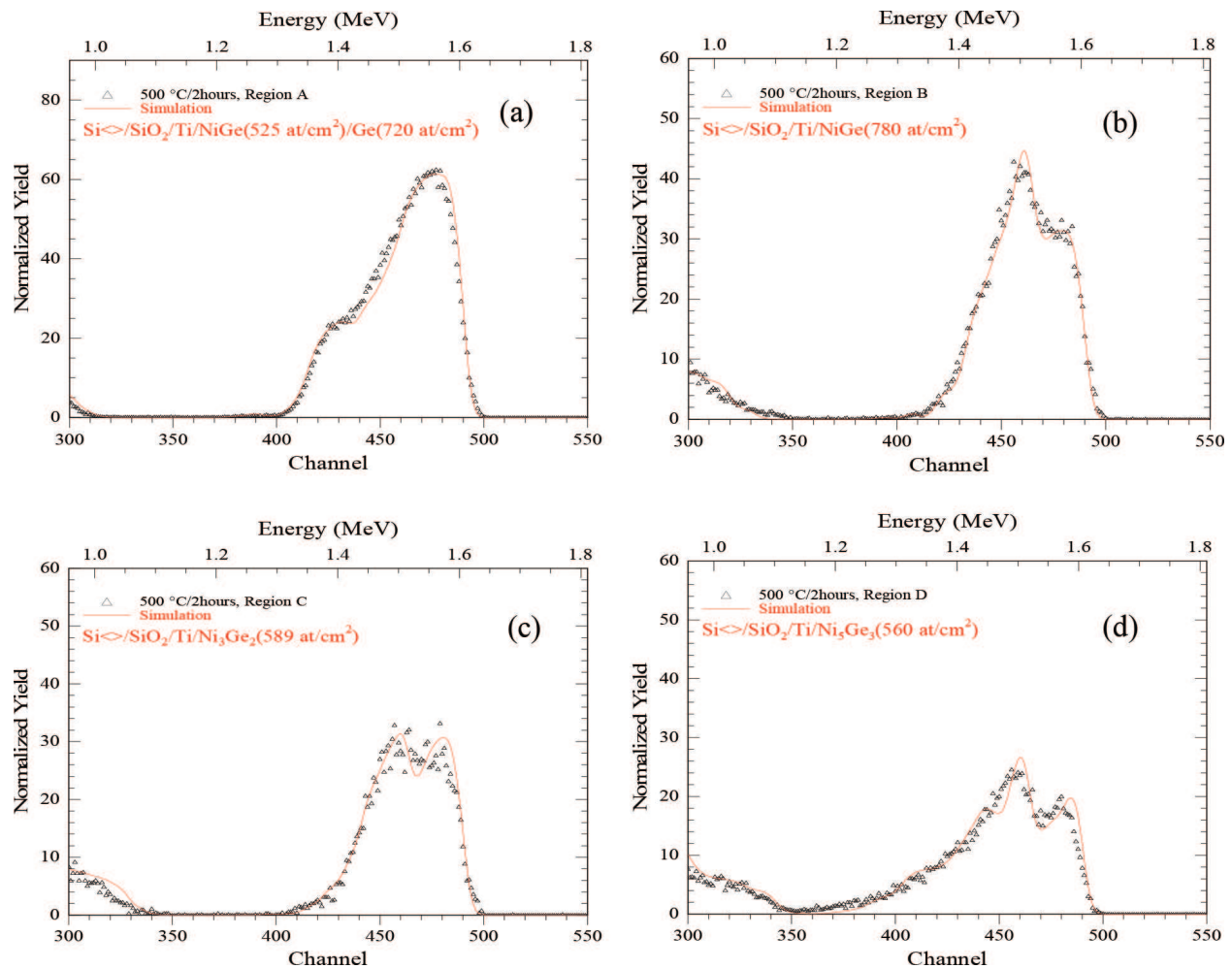
Figure 5. (a)–(d) show representative RBS spectra extracted from each of the four reaction regions A–D in the sample annealed at 500°C for 2 h, together with their RUMP simulations with thickness in units of 10^{15} atoms/cm^2.

3.2. Pd/Ge system

3.2.1. Thin film couples

The sputtered particles during the preparation of the thin film sample to investigate the relative contributions of each atomic species to the diffusion process in the Pd/Ge system had incident energies between 10 and 20 eV. This resulted in a degree of mixing of the sputtered particles with the substrate below the marker. It was detected using RBS analysis on the sample immediately after deposition (before any annealing) that some Pd atoms had penetrated through the atoms of the thin layer of W atoms into the region of the substrate Ge atoms. The configuration of the as-deposited sample was then: Ge(100)/Pd$_x$Ge/W(0.3 nm)/Pd(42.5 nm). After RUMP simulation of this sample, it was found that the Pd$_x$Ge layer could have been a 4 nm layer of Pd$_2$Ge. **Figure 6** shows the real-time RBS results during a ramped anneal at a rate of 1°C/min.

A schematic diagram summarizing results obtained is shown in **Figure 7**.

As the reaction commenced at around 150°C, the phase Pd$_2$Ge was formed on both sides of the marker as shown in **Figure 7(b)**. PdGe was formed around 180°C below the marker
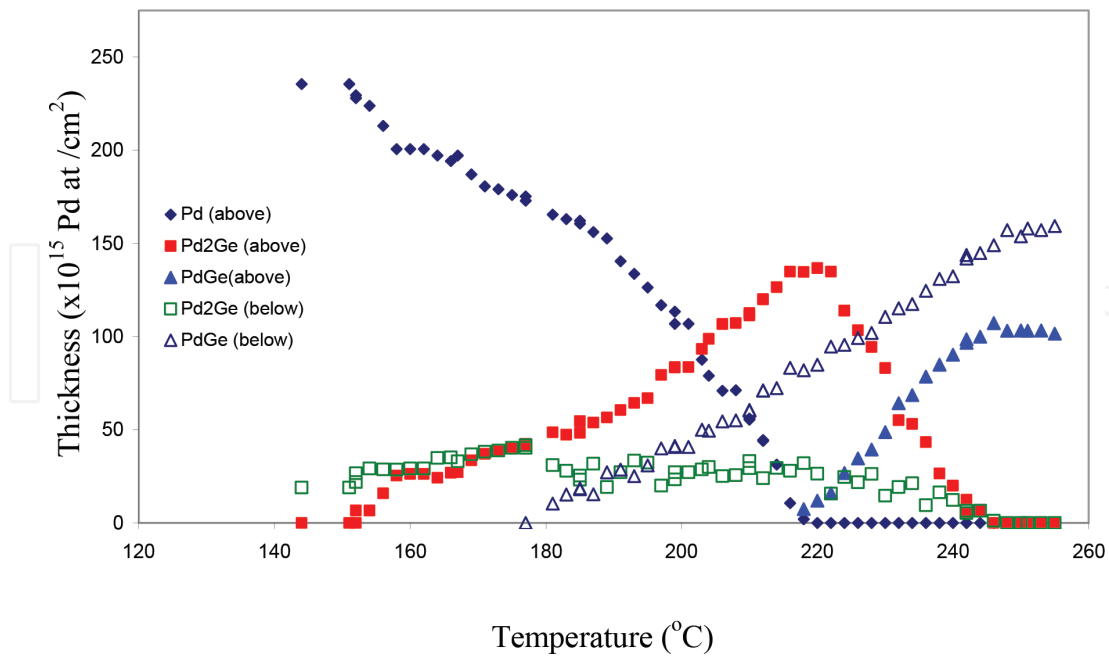
Figure 6. Plot showing the thickness of the various layers during the ramped thermal annealing of the Ge(100)/W/Pd sample. Pd_2Ge growth above and below the marker commences around 150°C. The PdGe phase first appears below the marker at around 180°C, and it appears above the marker at around 220°C, once all the Pd has been consumed [35].

between the Ge substrate and Pd_2Ge and Ge substrate, as shown in **Figure 7(c)**. It can be seen from **Figure 6** that Pd_2Ge was slightly consumed during the initial growth stages of PdGe. As temperature was increased, Pd_2Ge continued to grow above the marker while PdGe grew below the marker. At a temperature of around 220°C, the unreacted Pd was completely consumed and most of the phase below the marker was PdGe as shown in **Figure 7(d)**. The next stage of the reaction was the conversion of Pd_2Ge above the marker into PdGe. Above 220°C, the phase PdGe was present both below and above the marker as seen in **Figure 6**. **Figure 6** also shows that the reaction ended at a temperature of around 250°C.
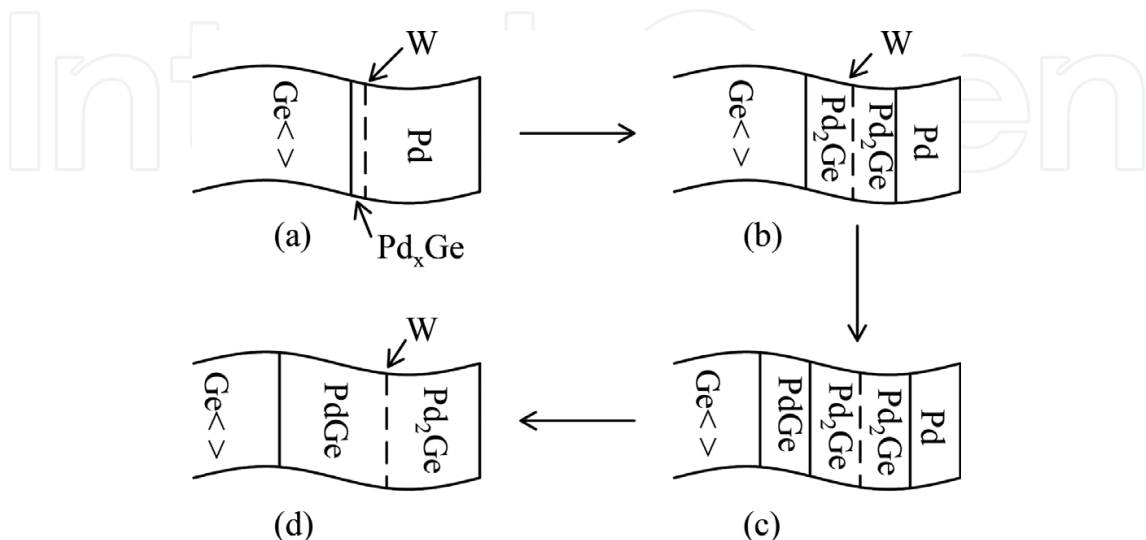

Figure 7. Schematic diagram summarizing the results obtained during the ramped thermal anneal of the Ge(100)/W/Pd sample.

3.2.2. Lateral diffusion couples

Samples for the lateral diffusion study of the Pd/Ge system were prepared by deposition of Ge islands (100 nm thick) on Pd films (20 nm thick). This configuration was chosen because the lateral diffusion couple results with Pd islands on Ge films showed little lateral diffusion upon annealing with a reaction region that was too narrow to resolve and monitor properly, indicating that Pd was not the DDS during lateral phase growth in the Pd/Ge system. Several lateral diffusion samples were annealed at various temperatures for different lengths of time. The Pd/Ge system exhibited relatively low temperature reaction. It was therefore necessary to carry out the investigation for this system at much lower temperatures than those used for the Ni/Ge systems. **Figure 8** shows an SEM micrograph of one representative sample with a 100 nm thick Ge island on a 20 nm thick Pd film, annealed at 325°C for 2 h, showing three distinct regions labeled A–C.

Areas which were chosen to include all the reaction regions observed were scanned on the nuclear microprobe for analysis by μRBS. A spectrum picked from each of the three regions of the Pd/Ge lateral diffusion sample is shown in **Figure 9**.

The spectrum from region C shows a peak of unreacted Pd and no Ge. The peak height of the spectrum taken from the region B shows the phase Pd_2Ge. This phase is seen at the surface position. From the solid line in the figure, it can be seen that the region A consisted of unreacted Ge and PdGe.

The solid line shows the spectrum form the original island region. This spectrum has a Pd peak at the surface position indicating that there was some Pd at the surface of the original island region. The fact that this Pd peak has what is labeled as a shoulder in **Figure 9** means that there was much less Pd at the surface of the region than deeper down. It therefore means that the region consisted of PdGe in the depth of the sample but toward the surface the PdGe phase was mixed with unreacted Ge making the Pd concentration much less.
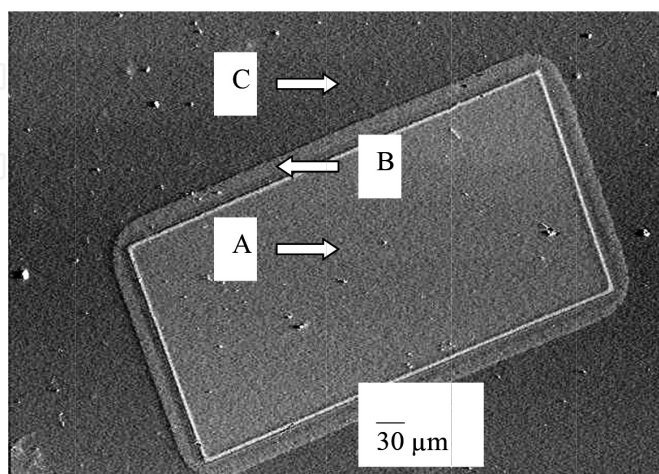

Figure 8. SEM micrograph of a Ge island (100 nm) on a Pd film (20 nm) annealed at 325°C for 2 h showing the different reaction regions.
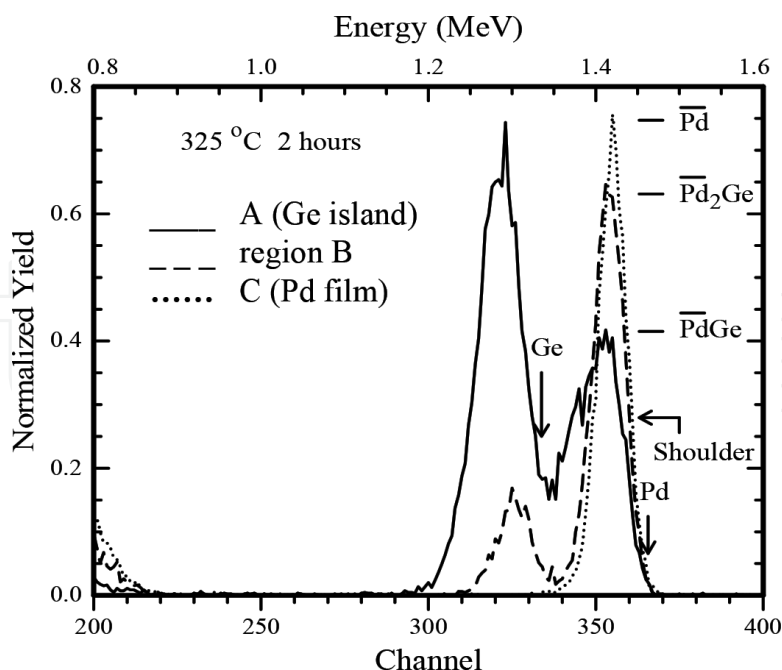
Figure 9. Superposition of selected RBS spectra from each of the regions of the Pd/Ge lateral diffusion sample. Pd peak heights of the various phases and surface positions of Ge and Pd are indicated.

4. Discussion

4.1. Thin film couples

The ideal case in marker studies is that the marker material should not have any effect on the formation of phases in the coupling materials. Ta and W appeared to be good choices of marker materials in that they did not react with Ge in the temperature ranges studied. An investigation was carried out during this work to see if the marker had any effect on the phase formation particularly at the beginning of the reaction. The temperature at which the reaction started in samples with a marker between the coupling layers was compared to the reaction onset temperature with no marker between the layers. It was found that the start of the reaction was delayed by a temperature of less than 10°C when the marker was present. This meant that although the marker acted as a sort of reaction barrier between coupling layers, its effect was not large enough to have any significant effect on the results of this study, in terms of the temperature of the first phase formation. Subsequent phases were expected to start forming when the supply of unreacted atoms to the growth interface reduced a level below some characteristic critical point [37]. The phase-formation sequence is not always expected to be straight forward because some cases of simultaneous phase growth have been report, as in the phases Ni_5Ge_3 and NiGe on Ge(100) substrates [38].

It was clear from the results of our thin film study that Ni was the only diffusing species during the formation of the first phase in the Ni/Ge system, Ni_5Ge_3. We now discuss the diffusing species during the formation of the second phase which is formed in the Ni/Ge system, NiGe.

It can be seen in **Figure 3** that the total amount (both reacted and unreacted) of Ni atoms/cm^2 remains constant throughout the reaction. One of the advantages of presenting the layer thickness in atoms/cm^2 units (as opposed to nm) is that this total amount remains constant for each element throughout the reaction, which provides an easy way of checking the consistency of the results at each temperature. It is seen in **Figure 3** that the reaction above the marker started at a much lower temperature than the reaction observed in the earlier marker investigation to establish the diffusing species during the formation of Ni_5Ge_3. It is likely that this is because in this case there is no Ta barrier between the coupling layers of Ni and Ge as was the case in the earlier investigation. In fact, room temperature reaction has been reported in the Ni/Ge system [39], in such a case where there is no barrier between the Ni and Ge layers.

The Ge above the marker was all converted in to Ni_5Ge_3 by the temperature of 250°C. The unreacted Ni then diffused across the marker to react with the Ge below. After the consumption of all the Ni, the Ni_5Ge_3 both below and above the marker both started to be converted into NiGe.

The conversion of Ni_5Ge_3 to NiGe above the marker could take place by either of the two reaction processes. Firstly, there is the decomposition reaction, $Ni_5Ge_3 \rightarrow 3NiGe + 2Ni$, where two Ni atoms are released, which then diffuse across the marker to react with the Ge in the substrate. If the NiGe formed below and above the marker were purely as a result of this reaction, then Ni would be the sole diffusing species during NiGe formation. This 100% Ni diffusion driven reaction would mean that three NiGe molecules would be formed above the marker for every two NiGe molecules formed below. A second possible reaction for the formation of NiGe above the marker is $Ni_5Ge_3 + 2Ge \rightarrow 5NiGe$. This would require that Ge diffuses across the marker to react with the Ni_5Ge_3 above. In all, we therefore see that the NiGe formed above the marker could be as a result of the diffusing of Ni, Ge, or both. The NiGe formed below the marker could only be due to Ni diffusion. In **Figure 10**, the NiGe formed above the marker is plotted against the total amount of NiGe formed.

Predicted plots for 100% Ni and 100% Ge diffusion are included as a dashed and dotted line respectively. The offset from the origin along the horizontal "total amount of NiGe" axis is
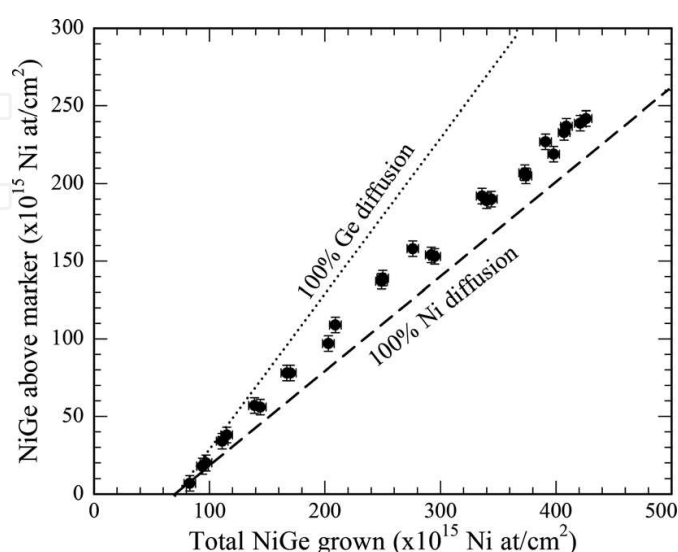

Figure 10. A plot of NiGe formed above the marker against the total amount of NiGe formed. Predicted plots for 100% Ni and 100% Ge diffusion are also included as a dashed and dotted line respectively [35].

because NiGe was initially formed by a reaction with unreacted Ni from the surface and not by the conversion of Ni_5Ge_3 into NiGe. It can be seen from **Figure 10** that both Ni and Ge diffuse during the formation of NiGe. The diffusion of Ge is dominant in the initial stages of the reaction but Ni diffusion becomes the prominent growth mechanism thereafter.

In our thin film study of the Pd/Ge system the results showed that during a large part of the reaction the W marker lay between two Pd_2Ge layers as shown in **Figure 7(c)**. This was before the total consumption of the unreacted Pd. Pd and Ge diffusion during the formation of Pd_2Ge can therefore be studied by monitoring the marker movement during this initial period. This part of the analysis does not include the reaction after all the Pd is consumed. Interestingly we will demonstrate later that the reaction after all Pd is consumed can be used to study the diffusing species during the formation of the second phase, PdGe.

Figure 11 shows the growth of Pd_2Ge above the maker as plotted against the Pd_2Ge formed below which also took into account the Pd_2Ge which had been converted into PdGe.

The three initial data points have been excluded during the plotting of the dashed line in **Figure 11**. This is because the initial stages of the reaction were complicated by the Pd which was deposited below the W marker during the sputter deposition. When one takes into account the fact that one Ge atom which diffuses across the marker forms one Pd_2Ge molecule above the marker whereas it takes two Pd atoms to diffuse across the marker to form one Pd_2Ge molecule below, then the best fit straight line through the data in **Figure 11** corresponds to Ge diffusion of about 40% and Pd diffusion of 60%.

If we look back at **Figure 7(d)** we see that this is the sample configuration at the point when the unreacted Pd is totally consumed. **Figure 7(d)** shows the marker at a position between PdGe and Pd_2Ge. There are two possible ways in which the reaction above the marker could proceed after this point. The first is for Ge atoms from the substrate below to diffuse across the marker
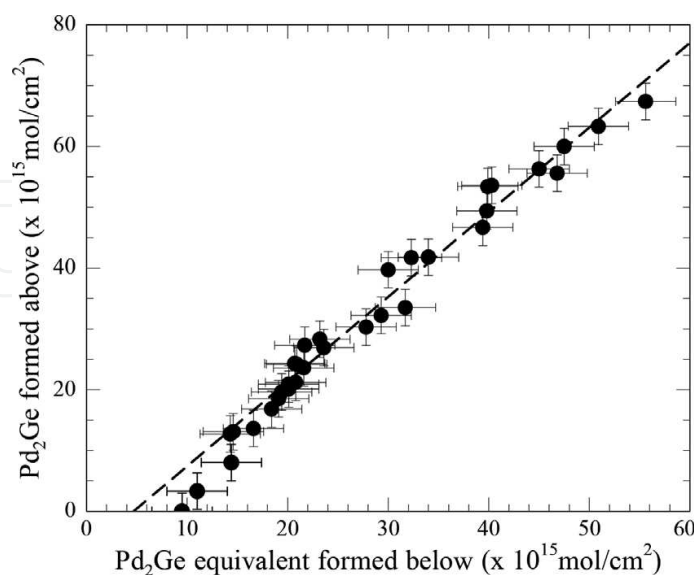

Figure 11. The growth of Pd_2Ge above the maker plotted against the Pd_2Ge formed below which also takes into account the Pd_2Ge which had been converted into PdGe. The dashed line, drawn through the uniform region (i.e., the line excludes the initial three data points), indicates that Pd is the dominant diffusing species during Pd_2Ge growth with a contribution of about 60%.

and react with Pd_2Ge converting it into PdGe. The other reaction could be the breaking down of Pd_2Ge producing PdGe and Pd. The Pd could then diffuse across the marker to react with the Ge below forming PdGe. We therefore get PdGe both below and above the marker, this is seen in **Figure 6**. The data acquired during the stage of the reaction after all Pd was consumed can therefore be used to study the diffusing species during the formation of PdGe. According to the reaction, $Pd_2Ge + Ge \rightarrow 2PdGe$, every Ge atom that diffuses across the marker from below will produce two PdGe molecules above the marker. From $Pd_2Ge \rightarrow PdGe + Pd$, we see that every Pd atom that diffuses across the maker from above will leave a PdGe molecule above and form another one below the marker. Any increase in the total amount of Ge above the marker could only be due to Ge diffusion from below. Any increase in the total amount of Pd below the marker could only be due to Pd diffusion from above. **Figure 12** is a plot of the total amount of Ge above the marker versus the total amount of Pd below the marker during the stage of the reaction after all unreacted Pd was consumed.

More scatter in found in this data set than for Pd_2Ge growth, but because of the relatively large number of readings obtained during real-time growth of the final phase the uncertainty is reduced, with the plot giving $65 \pm 3\%$ Pd diffusion during PdGe growth.

4.2. Lateral diffusion couples

As seen in **Figure 4(a)** and **(b)**, the interface between the regions C (consisting Ni_3Ge_2) and D (consisting of Ni_5Ge_3) was not distinct in the SEM and optical micrographs. It could only be determined using microprobe RBS. The available "beam time" on the microprobe was however not sufficient to analyze all our lateral diffusion samples. The growth lengths of these two regions were therefore combined during our analysis of the growth kinetics. Plots of reaction length against annealing time for the temperatures 300, 400, and 500°C were made. **Figure 13** shows the plot for 400°C.
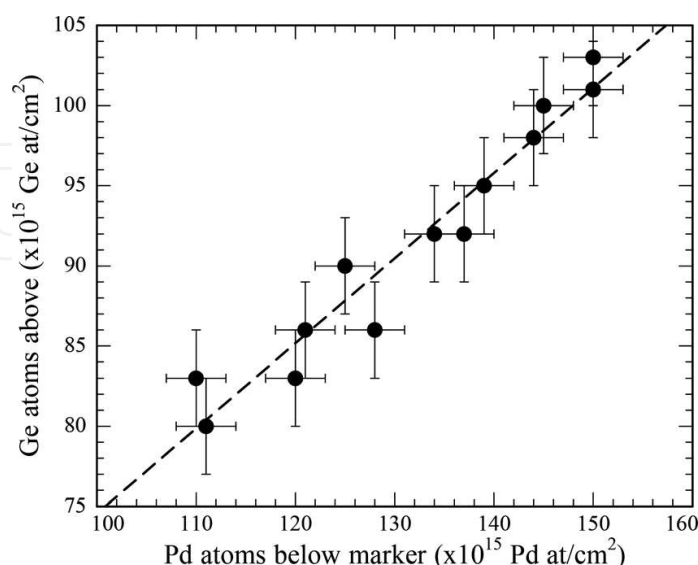

Figure 12. A plot of the total amount of Ge above the marker as a function of the total amount of Pd below the marker as Pd_2Ge transforms into PdGe, after all unreacted Pd is consumed. The gradient of the plot indicates that around 65% Pd diffusion took place during PdGe formation.
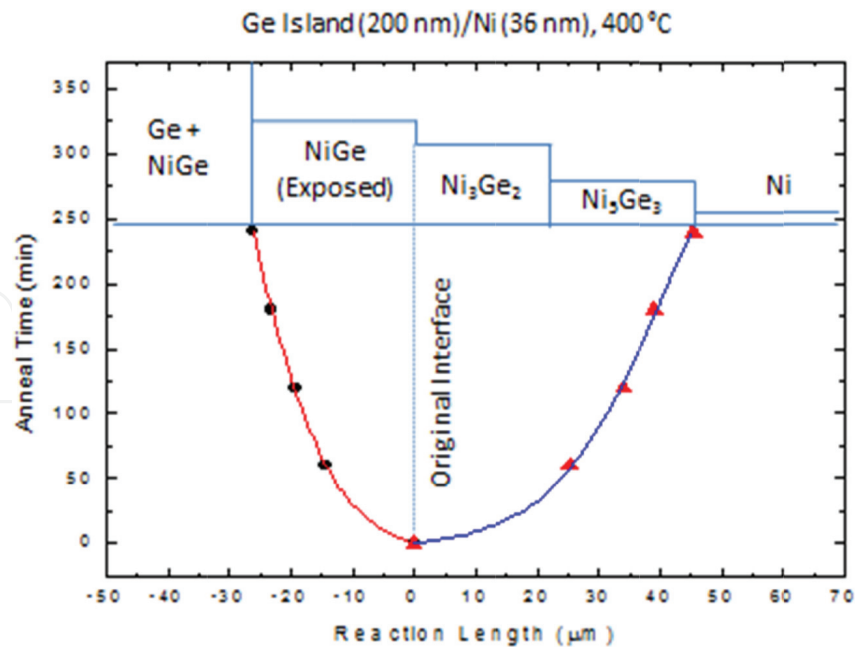
Figure 13. A plot of the reaction lengths of the phases against time of annealing at a temperature of 400°C. A parabolic dependence of compound growth with annealing time is observed.
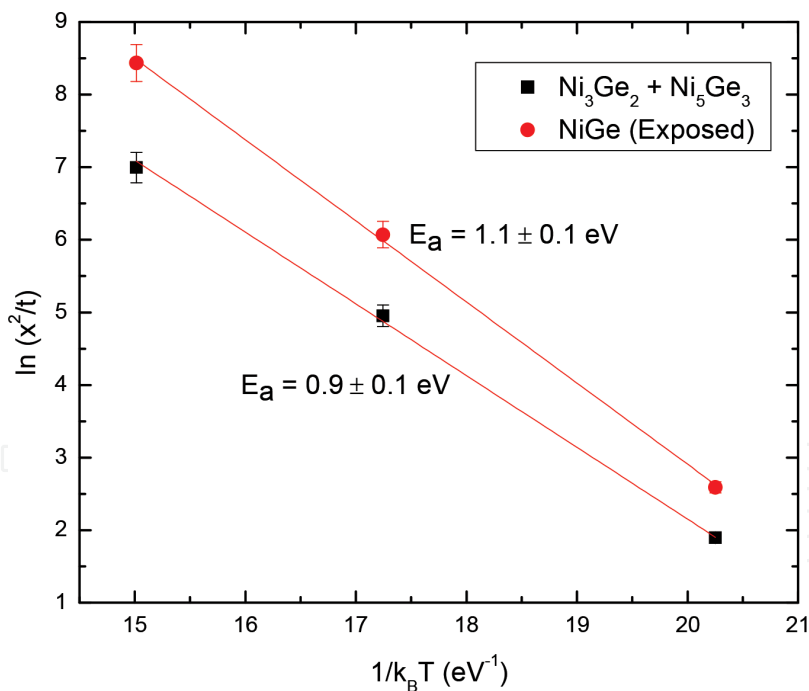

Figure 14. An Arrhenius plot for the combined lateral growth of Ni_3Ge_2 and Ni_5Ge_3 giving an activation energy of 0.9 ± 0.1 eV and another giving an activation energy of diffusion for Ge in NiGe as 1.1 ± 0.1 eV.

A parabolic dependence of compound growth with annealing time is observed. At every temperature, T the width, x_β of each phase region was measured. The values of the widths obtained were squared and plotted as a function of the corresponding periods of time, t that the samples were annealed for at the particular temperature. The slopes of these graphs gave the diffusional
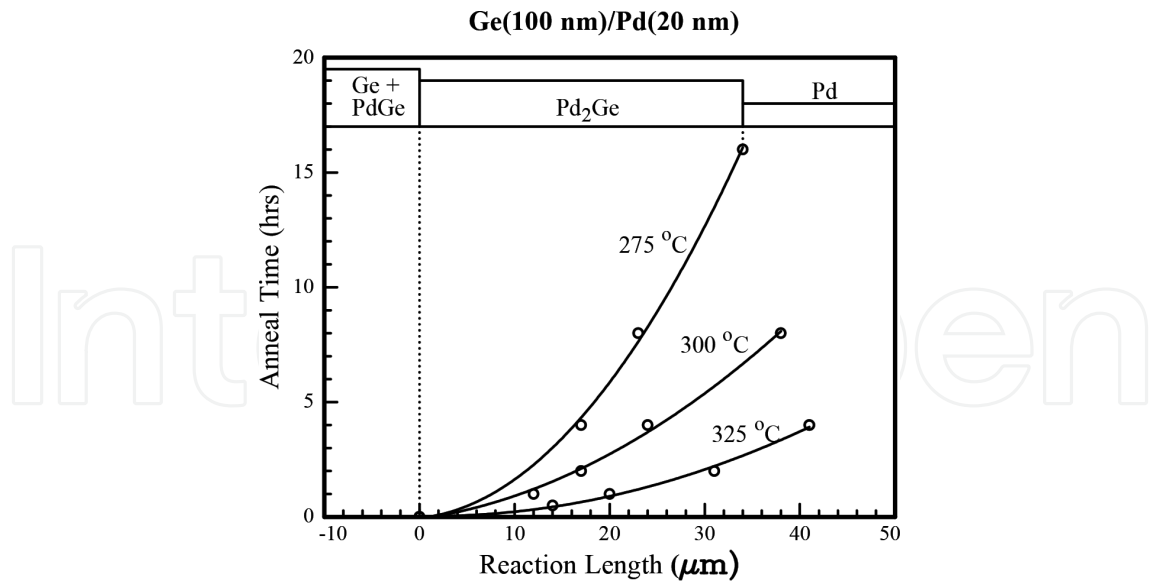
Ge(100 nm)/Pd(20 nm)

Figure 15. A plot of reaction length against the time of annealing for the phase Pd_2Ge at temperatures 275, 300, and 325°C.

growth constants, $K_\beta = x_\beta^2/t$. Arrhenius plots were then produced by plotting the logarithm of the diffusional growth constants versus the reciprocal of the product between the Boltzmann constant and the absolute temperature (i. e. $1/k_BT$), the results are presented in **Figure 14**.

From the slopes of these plots, the activation energy of diffusional growth for the combined lateral growth of Ni_3Ge_2 and Ni_5Ge_3 was determined to be 0.9 ± 0.1 eV while that corresponding to the rate of exposure of NiGe was 1.1 ± 0.1 eV.

The two phases, PdGe and Pd_2Ge, which were observed to form in the thin film study of the Pd-Ge system were also the only two observed in the lateral diffusion couples. The growth region outside the original island interface, labeled as region B in **Figure 8**, consisted of the phase Pd_2Ge. The original island region, labeled as region A in **Figure 8**, consisted of PdGe at the bottom while
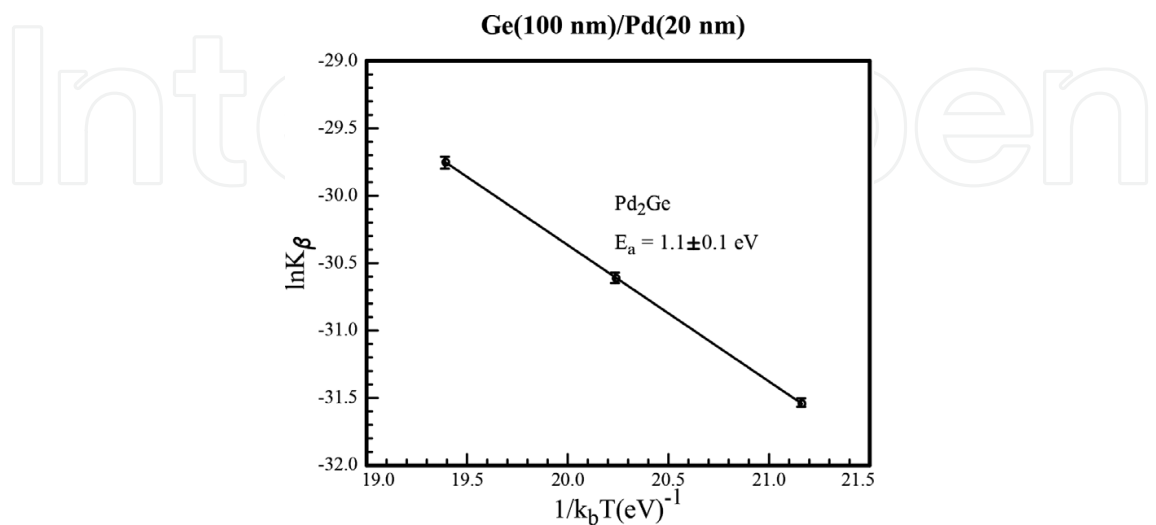
Ge(100 nm)/Pd(20 nm)

Figure 16. Arrhenius plot, $\ln K_\beta$ versus $1/k_bT$, showing temperature dependence of Ge diffusion rate through Pd_2Ge, yielding an average activation energy of 1.0 ± 0.1 eV.

at the top there was unreacted Ge intermingled with PdGe. There was only a very little and unworkable region of completely exposed PdGe without intermingled unreacted Ge, it was therefore not possible to obtained data for the growth or exposure rates of the phase PdGe. The growth of the Pd_2Ge region was monitored at the temperatures 275, 300, and 325°C. The periods of annealing were chosen so as to obtain a reasonable range of growth widths at each of the three temperatures; results are presented in **Figure 15**. Parabolic growth characteristics were observed.

Arrhenius plots were obtained from the data presented in **Figure 15**, in the same way as explained for the Ni/Ge lateral diffusion couples. **Figure 16** is an Arrhenius plot showing the temperature dependence of the Ge diffusion rate through Pd_2Ge.

The average activation energy determined from the plot in **Figure 16** was 1.0 ± 0.1 eV.

5. Conclusion

The movement of inert markers during the formation of palladium and nickel germanides was continuously monitored in conventional thin film couples using in situ RBS. The comparative contribution of each atomic species to the diffusion process during the formation of the phases was determined. Any changes of the comparative contributions of the atomic species during the phase growth process were studied. Ni_5Ge_3 and NiGe were observed to form in the Ni/Ge system with Ni_5Ge_3 being the first to form. Nickel was the only diffusing species during the formation of Ni_5Ge_3. Both Ni and Ge were observed to diffuse during the formation of NiGe. The diffusion of Ge was dominant in the initial stages of the reaction but Ni diffusion becomes the prominent growth mechanism thereafter. The only phases observed to form in the Pd/Ge system were PdGe and Pd_2Ge, the latter being the first. Both Pd and Ge are observed to diffuse during Pd_2Ge and PdGe formation. Palladium is however the dominant diffusing species during both Pd_2Ge and PdGe formation, being responsible for around 60% of the diffusion during Pd_2Ge formation and 65% of diffusion during PdGe formation. The results obtained for the first phase formation are in agreement with previously reported data. To the best of our knowledge this is the first time that the dominant diffusing species during NiGe and PdGe formation has been quantitatively determined, as mentioned earlier NiGe and PdGe are the most promising candidates for ohmic contacts in germanium-based technology [2, 3]. Our conventional thin film investigation has shown that the metal is the dominant diffusing species during the formation of the first phase. This is in agreement with the Cu_3Au ordered rule [40] which states that the majority diffusing element in an intermetallic ordered structure is the one with the highest diffusion coefficient. This rule was however not applicable to lateral diffusion couples.

Table 2 summarizes our results for the thin film and lateral diffusion couples in terms of the phase-formation sequences, phase-formation temperatures and diffusing species during the respective phase growths.

As presented in **Table 1**, the formation of Ni_5Ge_3 and NiGe was a common feature in the thin film and lateral diffusion couple results. However, Ni_3Ge_2 was only observed in lateral diffusion couple samples. Lateral diffusion couples provide a qualitative pointer to the dominant diffusing species in a system, without the need to interpose markers between coupling layers.

Phase - formation characteristics	Thin film couples		Lateral diffusion couples	
Phases observed	Ni_5Ge_3, NiGe, Pd_2Ge, PdGe		NiGe, Ni_3Ge_2, Ni_5Ge_3, Pd_2Ge, PdGe	
Phase-formation sequence	1st	Ni_5Ge_3, Pd_2Ge	Simultaneous lateral growth of phases	
	2nd	NiGe, PdGe		
Phase-formation temperatures	Ni_5Ge_3	150°C	Lateral reactions commenced at around 300°C in both the Ni/Ge and Pd/Ge systems	
	Pd_2Ge	140–150°C		
	NiGe	250°C		
	PdGe	180°C		
Diffusing species	Ni_5Ge_3	Ni	Combined growth of Ni_3Ge_2/Ni_5Ge_3	Ge
	NiGe	Ni is the DDS; Ge diffusion observed during the early stages of growth.	Exposure of NiGe	Ge
	Pd_2Ge	60% Pd and 40% Ge	Limited exposure of Pd_2Ge	Ge
	PdGe	65% Pd and 35% Ge	PdGe	Ge

Table 2. Summary of the results for the thin film and lateral diffusion couples in terms of the phase-formation sequences, phase-formation temperatures and diffusing species during the respective phase growths in the Ni/Ge and Pd/Ge systems.

The results from both diffusion couples with Ni islands on a Ge film and vice-versa indicate that Ge was the dominant diffusing species during germanide growth. The growth in the lateral diffusion couples was found to obey the $t^{1/2}$ law, indicating a diffusion-controlled process. The magnitude of the activation energy of the combined lateral growth of Ni_3Ge_2 and Ni_5Ge_3 was found to be 0.9 ± 0.1 eV, and that of the rate of exposure of NiGe was 1.1 ± 0.1 eV. The two phases, PdGe and Pd_2Ge, which were observed to form in the thin film study of the Pd/Ge system were also the only two observed in the lateral diffusion couples. The average activation energy determined for the lateral growth of Pd_2Ge is 1.0 ± 0.1 eV. The magnitudes of the activation energies calculated for all phases in this study suggest that the lateral diffusion reactions were not driven by surface diffusion but rather by diffusion through the interior of the lateral diffusion couples; typical values for surface diffusion being around 0.6 eV [41].

Acknowledgements

Author details

Adrian Habanyama[1]* and Craig M. Comrie[2]

*Address all correspondence to: adrian.habanyama@cbu.ac.zm

1 Department of Physics, Copperbelt University, Kitwe, Zambia

2 Department of Physics, University of Cape Town, Rondebosch, South Africa

References

[1] Brunco DP, De Jaeger B, Eneman G, Mitard J, Hellings G, Satta A, Terzieva V, Souriau L, Leys FE, Pourtois G, Houssa M, Winderickx G, Vrancken E, Sioncke S, Opsomer K, Nicholas G, Caymax M, Stesmans A, Van Steenbergen J, Mertens PW, Meuris M, Heyns MM. Germanium MOSFET devices: Advances in materials understanding, process development and electrical performance. Journal of the Electrochemical Society. 2008;**155**: H552-H561

[2] Gaudet S, Detavernier C, Kellock AJ, Desjardins P, Lavoie C. Thin film reaction of transition metals with germanium. Journal of Vacuum Science and Technology. 2006; **A24**:474

[3] Kittl JA, Opsomer K, Torregiani C, Demeurisse C, Mertens S, Brunco DP, Materials Science and Engineering. 2008;**144**:B154-B155

[4] Hökelek E, Robinson GY. A comparison of Pd Schottky contacts on InP, GaAs and Si. Solid State Electronics. 1981;**24**:99

[5] Rhoderick EH, Williams RH. Metal-Semiconductor Contacts. Oxford: Clarendon Press; 1988

[6] Baraff GA, Schlüter M. Binding and formation energies of native defect pairs in GaAs. Physical Review B. 1986;**33**:7346

[7] Asubay A, Güllü Ö, Türüt A. Determination of the laterally homogeneous barrier height of thermally annealed and unannealed Au/p-InP/Zn-Au Schottky barrier diodes. Applied Surface Science. 2008;**254**:3558

[8] Peng CY, Yang YH, Lin CM, Yang YJ, Huang CF, Liu CW. Process strain induced by nickel germanide on Ge substrate. In: 9th International Conference on Solid-State and Integrated Circuit Technology (ICSICT) Proceedings. 2008. pp. 681-683

[9] Hallstedt J, Blomqvist M, Persson POA, Hultman L, Radamson HH. The effect of carbon and germanium on phase transformation of nickel on $Si_{1-x-y}Ge_xC_y$ epitaxial layers. Journal of Applied Physics. 2004;**95**:2397

[10] Thanailakis A, Northrop DC. Metal-germanium Schottky barriers. Solid State Electronics. 1973;**16**:1383-1389

[11] Jin LJ, Pey L, Choi WK, Fitzgerald EA, Antoniadis DA, Pitera AJ, Lee ML, Chi DZ, Tung CH. The interfacial reaction of Ni with (111) Ge, (100) $Si_{0.75}Ge_{0.25}$ and (100) Si at 400 °C. Thin Solid Films. 2004;**462**:151-155

[12] Nemouchi F, Mangelinck D, Bergman C, Clugnet G, Gas P. Simultaneous growth of Ni_5Ge_3 and NiGe by reaction of Ni film with Ge. Applied Physics Letters. 2006;**89**:131920

[13] Patterson JK, Park BJ, Ritley K, Xiao HZ, Allen LH, Rockett A. Kinetics of Ni/a-Ge bilayer reactions. Thin Solid Films. 1994;**253**:456-461

[14] Gaudet S, Detavernier C, Lavoie C, Desjardins P. Reaction of thin Ni films with Ge: Phase formation and texture. Journal of Applied Physics. 2006;**100**:034306

[15] Majni C, Ottaviani G, Zani A. Growth kinetics of Pd_2Ge and PdGe. Journal of Non-Crystalline Solids. 1978;**29**:301

[16] Knaepen W. Characterization of solid state reactions and crystallization in thin films using in situ X-ray diffraction. [PhD thesis] Ghent: University of Ghent; 2010

[17] Scott DM, Pai CS, Lau SS. Thin film reaction investigation by backscattering spectroscopy – W Marker Study of Pd_2Ge formation. Proceedings of the Society of Photographic Instrumentation Engineers (SPIE). 1984;**463**:40-45

[18] Marshall ED, Wu CS, Pai CS, Scott DM, Lau SS. Metal-germanium contacts and germanide formation. Materials Research Society Symposium Proceedings. 1985;**47**:161

[19] Brunco DP, Opsomer K, De Jaeger B, Winderickx G, Verheyden K, Meuris M. Observation and suppression of nickel germanide overgrowth on germanium substrates with patterned SiO_2 structures. Electrochemical and Solid-State Letters. 2008;**11**:H39-H41

[20] Zhang SL, Ostling M. Metal silicides in CMOS technology: past, present and future trends. Critical Reviews in Solid State and Materials Sciences. 2003;**28**:1

[21] Nemutudi RS, Comrie CM. Churms CL. Study of Pt/Ge interactions in a lateral diffusion couple by microbeam rutherford backscattering spectrometry. Thin Solid Films. 2000;**358**:270

[22] Zheng LR, Hung LS, Mayer JW, Majni G, Ottaviani G. Lateral diffusion of Ni and Si through Ni_2Si in Ni/Si couples. Applied Physics Letters. 1982;**41**:646

[23] Zheng LR, Hung LS, Mayer JW. Silicide formation in lateral diffusion couples. Journal of Vacuum Science and Technology. 1983;**A1**:758

[24] Zheng LR, Hung LS, Mayer JW. Lateral diffusion of platinum through Pt_2Si in Pt/Si. Thin Solid Films. 1983;**104**:207-213

[25] Chen SH, Zheng LR, Barbour JC, Zingu EC, Hung LS, Carter CB, Mayer JW. Lateral-diffusion couples studied by transmission electron microscopy. Materials Letters. 1984;**2**:469-476

[26] Blanpain B, Mayer JW, Liu JC, Tu KN. Kinetic description of the transition from a one-phase to a two-phase growth regime in Al/Pd lateral diffusion couples. Journal of Applied Physics. 1990;**68**:3259-3267

[27] Blanpain B, Mayer JW, Liu JC, Tu KN. Layered growth of the quasicrystalline decagonal Al_3Pd phase in Al/Pd lateral diffusion couples. Physical Review Letters. 1990;**64**:2671

[28] Blanpain B, Liu JC, Lilienfeld DA, Mayer JW. Simultaneous growth of a crystalline phase and a quasicrystalline phase in lateral Al-Pd diffusion couples. Philosophical Magazine Letters. 1990;**61**:21-27

[29] Liu JC, Mayer JW, Barbour JC. Phase formation of $NiAl_3$. Journal of Applied Physics. 1988;**64**:651

[30] Liu JC, Mayer JW, Barbour JC. Kinetics of $NiAl_3$ and Ni_2Al_3 phase growth on lateral diffusion couples. Journal of Applied Physics. 1988;**64**:656

[31] Liu JC, Mayer JW. Aluminum and Ni-silicide lateral reactions. Journal of Materials Research. 1990;**5**:334-340

[32] Ding PJ, Talevi R, Lanford WA, Hymes S, Murarka SP. Use of a raster microbeam to study lateral diffusion of interest to microelectronics. Nuclear Instruments & Methods B. 1994;**85**:17

[33] de Waal HS. The effect of diffusion barriers, stress and lateral diffusion on thin-film phase formation. [PhD thesis]. South Africa: University of Stellenbosch; 1999

[34] Doolittle LR. Algorithm for rapid simulation of Rutherford backscattering spectra. Nuclear Instruments and Methods B. 1985;**9**:344-351

[35] Comrie CM, Smeets D, Pondo KJ, van der Walt C, Demeulemeester J, Knaepen W, Detavanier C, Habanyama A, Vantomme A. Determination of the dominant diffusing species during nickel and palladium germanide formation. Thin Solid Films. 2012;**526**:261-268

[36] Chilukusha D, Pineda-Vargas CA, Nemutudi R, Habanyama A, Comrie CM. Microprobe PIXE study of Ni-Ge interactions in lateral diffusion couples. Nuclear Instruments and Methods in Physics Research B. 2015;**363**:161-166

[37] Vantomme A, Degroote S, Dekoster J, Langouche G, Pretorius R. Concentration-controlled phase selection of silicide formation during reactive deposition. Applied Physics Letters. 1999;**74**:3137-3139

[38] Perrin C, Mangelinck D, Nemouchi F, Labar J, Lavoie C, Bergman C, Gas P. Nickel silicides and germanides: Phases formation, kinetics and thermal expansion. Materials Science and Engineering. 2008;**154**:163

[39] Smith GA, Luo L, Gibson WM. Ion channeling study of nickel metal growth on Ge<111> at room temperature. Journal of Vacuum Science and Technology. 1991;**A9**:646

[40] d'Heurle FM, Gas P, Lavoie C, Philibert J. Diffusion in intermetallic compounds: The ordered Cu_3Au rule, its history. Zeitschrift für Metallkunde. 2004;**95**:852-859

[41] Eckertova L. Physics of Thin Films. 2nd ed. New York: Plenum Press; 1986